www.czasopisma.pan.pl PAN POLSKA AKADEMIA NAUK www.journals.pan.pl

PAN ARCHIVES OF ACOUSTICS
Vol. **38**, No. 3, pp. 425–432 (2013)

DOI: 10.2478/aoa-2013-0050

A Clamped Bar Model for the Sompoton Vibrator

Tee Hao WONG[(1)], Jedol DAYOU[(1)], M.C.D. NGU[(1)], Jackson H.W. CHANG[(1)], Willey Y.H. LIEW[(2)]

[(1)] *Energy, Sound and Vibration Research Group (e-VIBS)*
School of Science and Technology, University Malaysia Sabah
Jalan UMS, 88400 Kota Kinabalu, Sabah, Malaysia; e-mail: jed@ums.edu.my

[(2)] *School of Engineering and Information Technology, University Malaysia Sabah*
Jalan UMS, 88400 Kota Kinabalu, Sabah, Malaysia

(*received May 8, 2012; accepted March 22, 2013*)

The sompoton is one of famous traditional musical instruments in Sabah. This instrument consists of several parts with the vibrator being the most important one. In this paper, the vibrator is modeled as a clamped bar with a uniformly distributed mass. By means of this model, the fundamental frequency is analyzed with the use of an equivalent single degree of freedom system (SDOF) and exact analysis. The vibrator is made of aluminum in different sizes and is excited using a constant air jet to obtain its fundamental resonance frequency. The fundamental frequency obtained from the experimental measurement is compared with the theoretical values calculated based on the equivalent SDOF and exact analysis theories. It is found that the exact analysis gives a closer value to the experimental results as compared to the SDOF system. Although both the experimental and theoretical results exhibit the same trend, they are different in magnitude. To overcome the differences in both theories, a correction factor is added to account for the production errors.

Keywords: vibrator, clamped bar, single degree of freedom system, exact analysis, resonance frequency.

1. Introduction

Malaysia is a developing country and Sabah is the second largest state which is richly blessed with natural diversity and unique heritages. It is important to preserve the cultural heritage at the same time moving towards a developed country. Malaysia is renowned for its cultural diverse indigenous communities of more than 30 ethnic groups. The largest ethnic group in Sabah is KadazanDusun. The sompoton undoubtedly belongs to their cultural heritage and it also serves as an attraction in tourism. This traditional musical instrument consists of three parts: the acoustic chamber, vibrator, locally known as sodi, and bamboo pipes (Fig. 1).

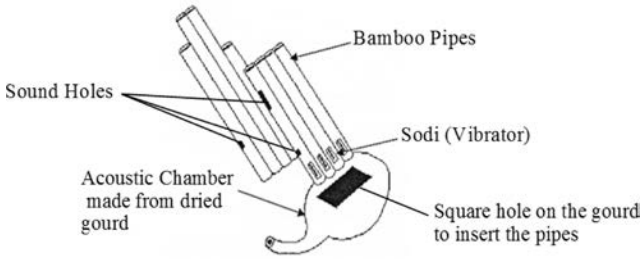

Fig. 1. Structure design of the sompoton (Marasan, 2003).

In the past, only a few studies scrutinized the sound production mechanism of musical instruments and even fewer studies dealt with traditional musical instruments. For example, Someya and Okamoto (2007) studied the measurement of the flow and vibration of the Japanese traditional bamboo flute using the dynamic PIV. They successfully visualized the air oscillation in the bamboo flute, which is useful to understand the important phenomena in sound production of the instrument. Rujinirum *et al.* (2005) characterized the acoustics properties for different types of wood used to make the Ranad (Thai traditional xylophone) and the resonator box. They managed to determine the dominant acoustic properties of the wood required to make good quality Ranad bars and resonator box. A wood with a high specific dynamic Young's modulus, density, and hardness is needed for the Ranad

box. As for the resonator box, a high value of acoustic converting efficiency (ACE) is necessary.

Far in the west Finland, Erkut *et al.* (2002) analyzed the sound generated by a Finnish traditional musical instrument known as the kantele, based on measurements and analytical formulation. A synthesis model had been proposed to capture the nonlinear properties of the kantele tones. The sounds produced were proven in accordance with the measurements and analytical approximations.

Due to the increasing demands for high quality sound production, a lot of research effort has been focused on the modern musical instruments. For instance, Fouilhe *et al.* (2011) managed to understand the changes of the cello's sound as the tailpiece characteristics changes. They successfully identified 9 different vibration modes and the effects of the tailpiece shape and types of attachments to the sound characteristics. Carral *et al.* (2011) made a comparison between the single reed and double reed mouthpieces of oboe. Both mouthpieces were played by a professional player and the sound produced was compared and studied. Lohri *et al.* (2011) investigated the appearances of combination tones in violins by recording the sound using two methods – two tones played simultaneously by a violinist, and excited using shakers. The outcome of the study opens up some further questions regarding the significance of combined tones in the string instrument and its performance.

Skrodzka *et al.* (2011) performed the modal analysis and laser Doppler vibrometry (LDV) measurements of the bracing pattern of the soundboard on two incomplete and complete guitars. Their investigation outcome showed that the bracing pattern does not affect at least the first three low frequencies mode shape of the incomplete/complete guitars. However, it does affect the modal frequencies of the instruments.

In the western part of Malaysia, Ismail *et al.* (2006) studied the properties and characteristics of the sound produced by a Malay traditional musical instrument – the kompang and analyzed them using computer music synthesis. The kompang is noted as a pitchless musical instrument and it is similar to other vibrating circular membrane instruments. Similar research on pitchless instruments dedicated to the modal analysis of the batter head of the snare drum was done by Skrodzka *et al.* (2006). They performed measurements of the instrument's sound spectrum. The results showed that the batter head is not the strongest radiating element of the drum system, and the influence of other elements may also have a significant role in the sound radiation. In Sabah (east Malaysia), Ong and Dayou (2009) initiated the study of the frequency analysis of the sound from a local traditional musical instrument, the sompoton. They reported that the generation of harmonic frequency from the sompoton follows the open-end pipe model but the fundamental frequency does not comply with the same model.

The sompoton is played by blowing the air into the gourd (acoustic chamber) through the mouthpiece (Fig. 2). The air resonance in the gourd then acts as an airjet passing through the vibrator making it to vibrate and thus producing audible sound. Musicians can produce a melody by covering and uncovering the opening of the three shorter pipes with their right hand and small sound holes near the front and back pipes with their left hand.

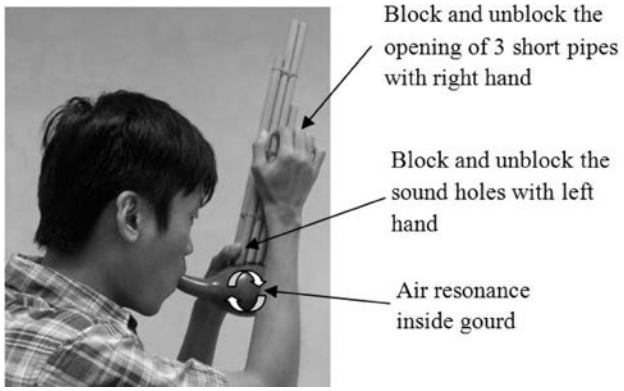

Fig. 2. Standard posture while playing the sompoton.

Up till now, very limited studies have considered the vibrator of the sompoton. In view of this, it is important to expand the studies in the effort to preserve this traditional musical instrument. The vibrator plays an important role in the sound production by the sompoton. The original vibrator is made of polod which is a kind of a palm tree found locally. The existing vibrator does not have fixed standard dimensions to produce a certain sound frequency. It depends on the expertise of the master. In this research, the vibrator is constructed using aluminum instead of polod, to provide a less complicated way to understand the sound production mechanism of the sompoton. To carry out this work, vibrators of different dimensions were produced and analyzed in order to determine the governing formulation of the fundamental frequency.

2. Clamped bar model and fundamental frequency analysis of the vibrator

2.1. Rayleigh's energy theory and SDOF system analysis

A clamped bar in mechanical constructions is called a cantilever beam, which is a bar supported at one end, whereas the other end can vibrate freely (Fig. 3a). It is widely found in construction designs such as cantilever bridges, balconies, and it is also applied in the aircraft wings design. Detailed inspection of the sompoton's vibrator in Fig. 3b shows that generally it has a similar design to the clamped bar (Fig. 3a), where one end of the vibrator is attached to the frame and the other end vibrates freely when it is subjected to a force.

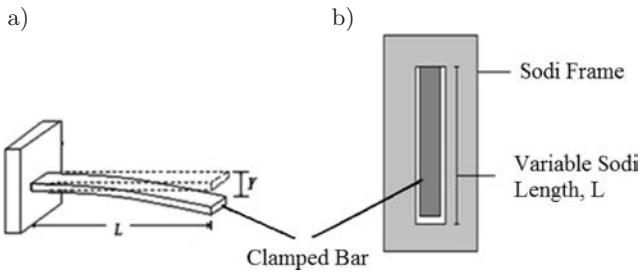

Fig. 3. Schematic diagram of the clamped bar and vibrator (sodi): a) clamped bar model, b) schematic drawing of the vibrator.

Although a clamped bar has many modes of vibration, the knowledge of its fundamental mode is of prime importance, as higher frequencies are the multiplication of this fundamental frequency. Therefore, in this paper, an equivalent single-degree-of-freedom system is adopted. The vibrator is modeled as a single mode clamped bar to predict its fundamental frequency.

The sompoton's vibrator has a uniform dimension and, therefore, can be modeled as a clamped bar with a uniformly distributed mass as shown in Fig. 4. When a uniformly distributed force is applied, Rayleigh energy theorem can be used to determine its fundamental sound frequency, according to which angular frequency of a vibrating system can be written as

$$\omega = \sqrt{\frac{k}{M}}\,, \tag{1}$$

where ω is the angular frequency in radian per second, k is the stiffness of the bar and M is the mass.

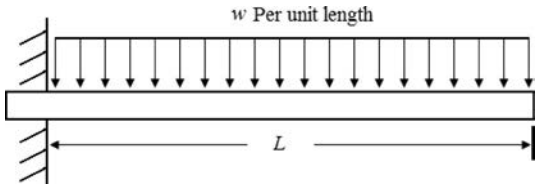

Fig. 4. Clamped bar of length L fixed at one end and carrying a uniformly distributed mass of w per unit length over the entire length of the bar.

The angular frequency can be expressed in the form of

$$\omega = 2\pi f. \tag{2}$$

Combining equation (1) and (2) gives

$$f = \frac{1}{2\pi}\sqrt{\frac{k}{M}}\,. \tag{3}$$

The maximum deflection of the clamped bar, y is given by (Gere, Goodno, 2009; Merriman, 1924)

$$y = \frac{wL^4}{8EI}\,, \tag{4}$$

where E is the modulus of elasticity, I is the second moment of inertia, L is the length, w is the uniform weight per unit length.

The stiffness of the bar system can be written as

$$k = \frac{F}{y} = \frac{wL}{y}\,, \tag{5}$$

where F is the total force acting on the bar.

Substitute Eq. (4) into Eq. (5) gives

$$k = \frac{8EI}{L^3}\,. \tag{6}$$

According to the Rayleigh energy theorem, the clamped bar system is analogous to the system of a spring mass. Therefore, the stiffness, k in Eq. (3) can be substituted by Eq. (6) to give the fundamental natural frequency of a uniformly distributed mass as

$$f = \frac{1}{2\pi}\sqrt{\frac{8EI}{ML^3}}\,, \tag{7}$$

where M is the mass of the bar which is calculated from the density value taken from the standard table of aluminum and L is the length of the bar.

2.2. Exact analysis

The free transverse vibration of the bar can be described as a differential equation of motion as

$$M\frac{\partial^2 y}{\partial t^2} + EI\frac{\partial^4 y}{\partial x^4} = 0, \tag{8}$$

where E, I, y, and M denotes Young modulus of elasticity, second moment of inertia, transverse deflection, and mass per unit length of the bar, respectively.

Using the method of separation of variables, we can write

$$\frac{EI}{M}\,\frac{1}{\varphi(x)}\,\frac{\mathrm{d}^4\varphi(x)}{\mathrm{d}x^4} = -\frac{1}{q}\,\frac{\mathrm{d}^2 q(t)}{\mathrm{d}t^2} = \omega^2, \tag{9}$$

where ω^2 is defined as constant.

This equation is then separated into separate differential equations as

$$\frac{\mathrm{d}^4\varphi(x)}{\mathrm{d}x^4} - \lambda^4\varphi(x) = 0, \qquad \frac{\mathrm{d}^2 q(t)}{\mathrm{d}t^2} + \omega^2 q(t) = 0, \tag{10}$$

where

$$\lambda^4 = \frac{\omega^2 M}{EI}\,. \tag{11}$$

The general solutions to the Eqs. (10) are

$$\begin{aligned} \varphi(x) &= C_1\cosh(\lambda x) + C_2\cos(\lambda x) \\ &\quad + C_3\sinh(\lambda x) + C_4\sin(\lambda x), \\ q(t) &= C_5\sin(\omega t) + C_6\cos(\omega t). \end{aligned} \tag{12}$$

Equation $(12)_1$ has four constants and requires four boundary conditions. For the case of a bar clamped at one end, the boundary conditions at the clamped end ($x = 0$) are that both deflection ($\varphi(x)$) and the

slope $(\partial\varphi(x)/\partial x)$ should be equal to zero. On the other hand, at the free end, the bending moment $EI(\partial^2\varphi(x)/\partial x^2)$ and shear force $EI(\partial^3\varphi(x)/\partial x^3)$must both be zero (Morse, 1948).

After substituting the four boundary conditions into the Eq. $(12)_1$ and arranging it into the matrix form we have:

$$\begin{bmatrix} 1 & 1 & 0 & 0 \\ 0 & 0 & 1 & 1 \\ \cosh(\lambda L) & -\cos(\lambda L) & \sinh(\lambda L) & -\sin(\lambda L) \\ \sinh(\lambda L) & \sin(\lambda L) & \cosh(\lambda L) & -\cos(\lambda L) \end{bmatrix} \times \begin{bmatrix} C_1 \\ C_2 \\ C_3 \\ C_4 \end{bmatrix} = \begin{bmatrix} 0 \\ 0 \\ 0 \\ 0 \end{bmatrix} \quad (13)$$

or simply $[Q][C] = [0]$.

The constant matrix $[C]$ cannot be equal to zero (otherwise no vibration is present). Therefore, the determinant of $[Q] = 0$. The result of the determinant gives

$$\cosh(\lambda L)\cos(\lambda L) + 1 = 0, \quad (14)$$

which is the frequency equation.

The first four solutions for a clamped bar free vibration are given as

$$(\lambda L)_1 = 1.875104, \quad (\lambda L)_2 = 4.694091,$$
$$(\lambda L)_3 = 7.854757, \quad (\lambda L)_4 = 10.9955.$$

When the first value $\lambda L = 1.8751$ is substituted into Eq. (11) and rearrangement of the equation gives the fundamental frequency

$$\omega = 1.0150\frac{h}{L^2}\sqrt{\frac{E}{\rho}} \quad (15)$$

or

$$v = 0.1615\frac{h}{L^2}\sqrt{\frac{E}{\rho}}, \quad (16)$$

which gives values in Hz.

3. Experimental setup, results, and discussion

The aim of this paper is to establish a theoretical model that can explain the sound production mechanisms of the sompoton. In the previous section, a hypothesis was proposed that the sompoton's vibrator is similar to a clamped bar due to the similarity in their structural designs. In this section, experimental works were performed to verify this hypothesis and investigate the governing factors that may affect the sound emitted by the vibrator. To do this, vibrators of different lengths were produced from thin aluminum plate using Computer Numerical Control (CNC) machine to ensure uniformity. The width and thickness of the produced vibrators is fixed at 2 mm and 0.2 mm, respectively.

Figure 5 shows the experimental setup of this work. The vibrator was excited by using constant air jet pressure from an air compressor. The bar of the vibrator acts as an air gate that alternately blocks and un-blocks the passing air. This generates a vibration in the surrounding air and thus produces an audible tone (Hopkin, 1996). The sound generated by excitation of the vibrator was recorded using the Harmonie measurement system and later analysed using MATLAB to obtain the frequency spectrum. To avoid unwanted noise, the experiments were carried out in a noise free anechoic room. The aluminium vibrator was made with the modulus of elasticity $E = 70$ GPa, second moment of inertia $I = 1.333 \times 10^{-15}$ Nm, and density $\rho = 2700$ kg/m^3. The values of the modulus of elasticity and density are taken from the standard table for aluminum.

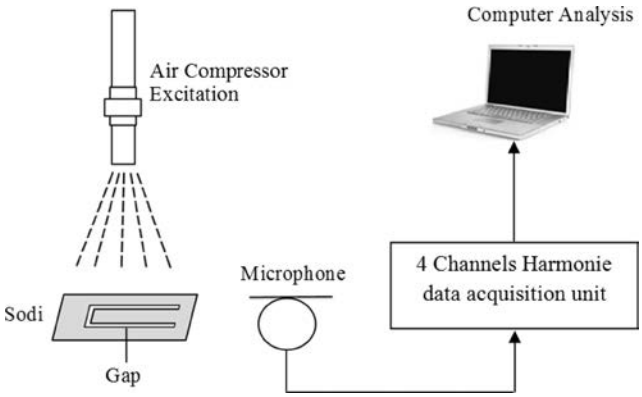

Fig. 5. Experimental setup of the sompoton's vibrator excitation and data analysis.

Table 1 shows the frequency values for different lengths of the vibrator obtained from the experimental measurements and theoretical calculation of SDOF system using Eq. (7). It should be noted that the sec-

Table 1. Experimental and theoretical value of SDOF fundamental frequency of the sound from aluminum vibrator.

Vibrator length L [mm]	Experimental frequency f_e [Hz]	SDOF system frequency f_t [Hz]	Percentage difference Δ [%]
17	572.0	457.9	19.95
18	567.0	408.4	27.97
19	520.0	366.6	29.50
20	505.7	330.8	34.59
21	413.0	300.1	27.34
22	392.4	273.4	30.33
23	359.0	250.2	30.31
24	338.0	229.8	32.01
25	304.1	211.7	30.38

ond moment of inertia I in the equation was calculated using the dimension of the aluminium vibrator, the mass M is the measured mass of the vibrator itself, and the length L is the length of the vibrator given in Table 1. It is clearly seen that both frequencies differ in magnitude. This is further visualized in a graphical comparison shown in Fig. 6 where the frequency obtained from measurement is always higher as compared to the theoretical value. Detailed inspection of Fig. 6 also shows that although they differ in magnitude, both data shared an identical trend – the sound frequency decreases as the vibrator length increases in a similar proportion. Errors occurring during production are a possible reason to explain the differences in the results. During the cutting process, the CNC machine's cutter defects the vibrator's bar and leaves a little curvature shape on the bar. Therefore, each vibrator experienced similar defects in production with the same proportion.

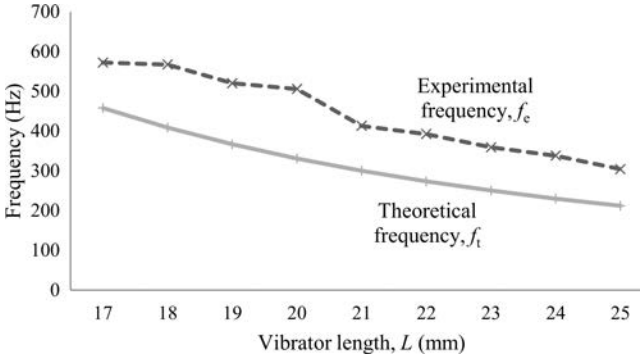

Fig. 6. Comparison between the theoretical SDOF using Eq. (7) and experimental values of the fundamental frequency of the aluminum vibrator of different lengths.

To account for the production errors, a correction factor must be added into the theoretical formula to determine the actual frequency. The linear scale graph in Fig. 6 is first rescaled into a semilog of y-axis as shown in Fig. 7.

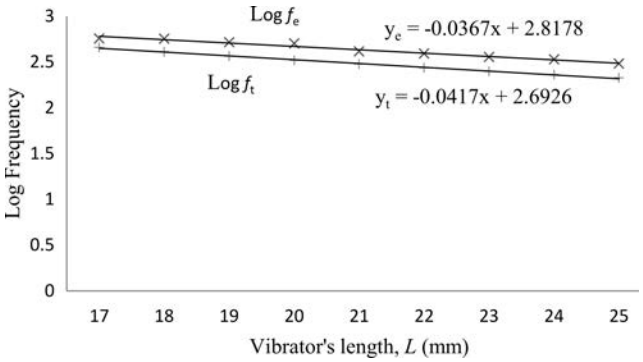

Fig. 7. Conversion of the graph in Fig. 6 into a logarithm form.

It can be seen now that the data obtained from the experimental work ($\log f_e$) and theoretical prediction ($\log f_t$) are in the linear proportion. For clarity, both equations are written in the following way:

$$\log f_e = -0.0367x + 2.817, \tag{17}$$

$$\log f_t = -0.0417x + 2.692. \tag{18}$$

Substituting Eq. (17) into (18) for x gives, after rearrangement:

$$\log f_t - 1.1362 \log f_e = -0.5091. \tag{19}$$

This can also be rewritten as

$$\log\left(\frac{f_t}{f_e^{1.1362}}\right) = -0.5091. \tag{20}$$

From the log identity, it can be written that

$$\frac{f_t}{f_e^{1.1362}} = 0.3097 \tag{21}$$

or

$$f_t = 0.3097 f_e^{1.1362}. \tag{22}$$

Rearranging the equation gives

$$f_e = \sqrt[1.1362]{3.229 f_t}, \tag{23}$$

which gives the final equation as

$$f_e = 2.81 f_t^{0.88}, \tag{24}$$

rounded to two decimal points, where f_t is the theoretical value of frequency of the produced vibrator given in Eq. (7).

Equation (24) relates the experimental and theoretical values of the vibrator's frequency. It is the corresponding equation that gives the actual frequency in terms of a theoretical equation with the correction factor. This means that using the same CNC machine setting, the required thickness of the vibrator has to be adjusted according to this equation and not to the theoretical formulation in Eq. (7).

In order to validate this new formula, the theoretical value of the frequency of the produced vibrator in Table 1 was substituted into Eq. (24) and then compared with the actual measurement. Table 2 shows the comparison between the two values. The table shows that the two set of values are in a close agreement with a maximum deviation of 8.37%. It can also be seen in Fig. 8 that the corrected frequency now closely matches the experimental frequency. Both graphs show a similar decreasing trend as the vibrator's length decreases.

In comparison with the previous analysis using the equivalent SDOF system, theoretical frequency values using the exact solution have been calculated. It was found that the fundamental frequency obtained from the exact analysis shows a closer agreement to the measured frequency. Comparing with the theoretical frequency derived from the SDOF system which shows

Table 2. Experimental and corrected SDOF formula result data of the aluminum vibrator length test.

Vibrator length L [mm]	Experimental frequency f_e [Hz]	Corrected formula frequency f [Hz]	Percentage difference Δ [%]
17	572.0	616.9	7.84
18	567.0	557.8	1.63
19	520.0	507.2	2.46
20	505.7	463.4	8.37
21	413.0	425.3	2.98
22	392.4	391.8	0.15
23	359.0	362.4	0.95
24	338.0	336.3	0.51
25	304.1	312.9	2.88

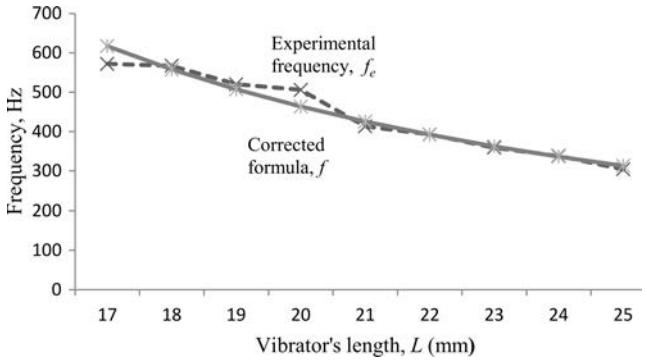

Fig. 8. Comparison graph of the experimental and corrected SDOF theoretical formula.

the maximum discrepancy of 34.59% (Table 1), the exact analysis gives a better result with the maximum discrepancy of 18.67% (Table 4). It can be clarified in Table 3 and Fig. 9 that the value from the exact analysis shows a closer match to the experimental value.

Table 3. Comparison of the fundamental frequency of the vibrator obtained using the SDOF system, exact analysis, and measurement.

Vibrator length L [mm]	Experimental frequency f_e [Hz]	SDOF system frequency f_t [Hz]	Exact solution frequency v [Hz]
17	572.0	457.9	569.2
18	567.0	408.4	507.7
19	520.0	366.6	455.7
20	505.7	330.8	411.3
21	413.0	300.1	373.0
22	392.4	273.4	339.9
23	359.0	250.2	311.0
24	338.0	229.8	285.6
25	304.1	211.7	263.21

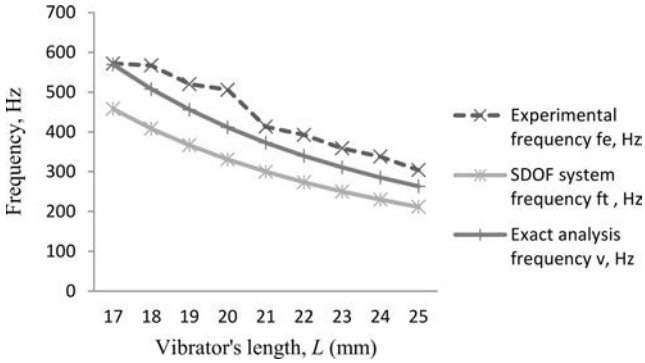

Fig. 9. Graphical comparison of the fundamental frequency of the vibrator obtained using the SDOF system, exact analysis, and measurement.

Table 4. Experimental and exact analysis values of the fundamental frequency of the sound of the aluminum vibrator.

Vibrator length L [mm]	Experimental frequency f_e [Hz]	Exact analysis frequency v [Hz]	Percentage difference Δ [%]
17	572.0	569.2	0.49
18	567.0	507.7	10.46
19	520.0	455.7	12.37
20	505.7	411.3	18.67
21	413.0	373.0	9.69
22	392.4	339.9	13.38
23	359.0	311.0	13.37
24	338.0	285.6	15.50
25	304.1	263.21	13.44

Figure 10 illustrates a graphical comparison of the frequencies obtained from the exact analysis and the measurement. It can be seen that the experimental value is always higher than the calculated frequency. A similar explanation from the SDOF analysis can be applied for the result differences as discussed before, where the production error could be the main reason for it.

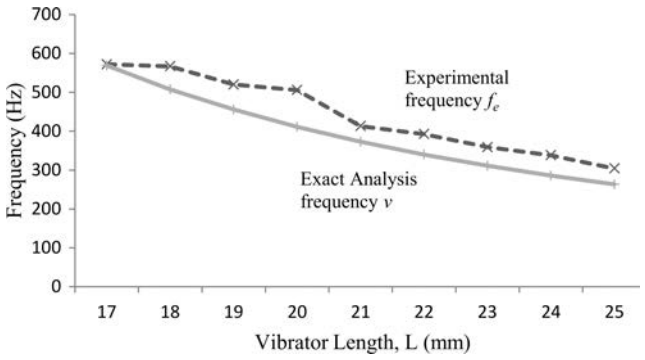

Fig. 10. Comparison of the exact analysis and experimental values of the fundamental frequency of the aluminum vibrator with a different length.

Therefore, a correction factor is also needed to account for the production errors in the exact analysis. Following a similar approach for the SDOF system, Fig. 10 is rescaled into a semilog y-axis graph which is shown in Fig. 11.

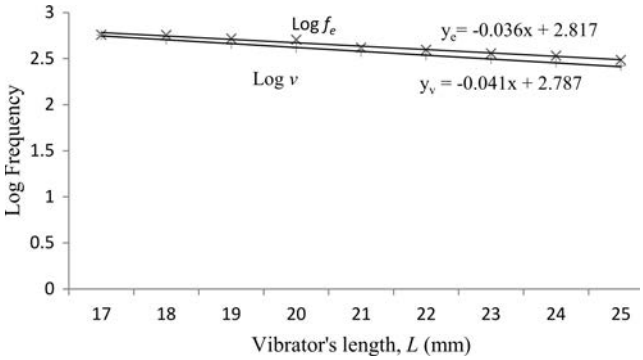

Fig. 11. Conversion of the exact solution graph into a logarithm form.

Using both linear equations from the logarithmic graph, the steps from Eq. (17) to Eq. (24) are then repeated to obtain the corrected formula for the exact analysis. The new corrected formula of the exact analysis obtained is

$$v_c = 2.34v^{0.88}\,. \tag{25}$$

Table 5 compares the corrected values of the exact analysis with the experimental frequency. It shows that both sets of values are now in a better agreement, where the maximum discrepancy is reduced to 8.76%. It can further be seen in Fig. 12 that the corrected frequency is now closely matched with the measured frequency.

Table 5. Comparisons between the measured and corrected exact solutions of the fundamental frequency of the aluminum vibrator.

Vibrator length L [mm]	Experimental frequency f_e [Hz]	Corrected formula frequency v_c [Hz]	Percentage difference Δ [%]
17	572.0	622.1	8.76
18	567.0	562.5	0.79
19	520.0	511.5	1.63
20	505.7	467.4	7.57
21	413.0	428.9	3.85
22	392.4	395.2	0.71
23	359.0	365.5	1.81
24	338.0	339.1	0.33
25	304.1	315.6	3.78

Table 6 summarises the work in this paper. It shows the comparison between the frequencies of the aluminium vibrator obtained from the corrected equivalent SDOF model and corrected exact solution, with

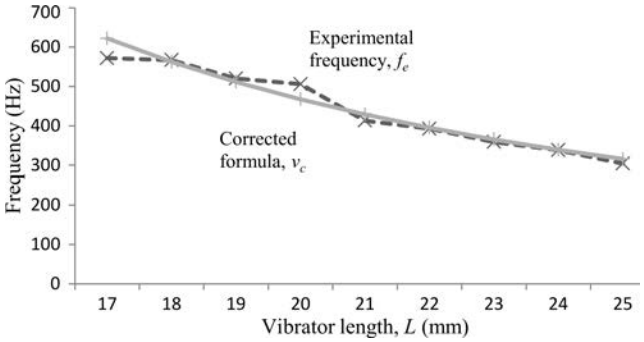

Fig. 12. Graphical comparisons between the experimental and corrected exact solutions of the fundamental frequency of the aluminum vibrator.

the actual value obtained by measurement. It can be seen that the percentage difference for both theoretical analyses with the correction factor has reduced and their values are closer to the measured fundamental frequency.

Table 6. Comparison, in percentage difference, between the frequencies obtained using corrected SDOF and corrected exact analysis, with the actual values.

Vibrator length L [mm]	Experimental frequency f_e [Hz]	SDOF frequency f [Hz]	Percentage difference Δ [%]	Exact analysis frequency v_c [Hz]	Percentage difference Δ [%]
17	572.0	616.9	7.84	622.1	8.76
18	567.0	557.8	1.63	562.5	0.79
19	520.0	507.2	2.46	511.5	1.63
20	505.7	463.4	8.37	467.4	7.57
21	413.0	425.3	2.98	428.9	3.85
22	392.4	391.8	0.15	395.2	0.71
23	359.0	362.4	0.95	365.5	1.81
24	338.0	336.3	0.51	339.1	0.33
25	304.1	312.9	2.88	315.6	3.78

4. Conclusions

This paper presented modeling of the sompoton's vibrator using a clamped bar model for the analysis of the fundamental resonance frequency. Several sompoton's vibrators made of aluminum thin plate of different length were produced using the Computer Numerical Control (CNC) machine to ensure uniformity. The equivalent single degree of freedom system (SDOF) and exact solutions were then used as a theoretical analysis method. It was found that exact formulation provides a better prediction of the vibrator's fundamental frequency as compared with the experimental measurement. However, both theoretical analysis models (the SDOF and exact analysis) show a certain per-

centage of deviation from the actual measurement. To solve the problem, a correction factor for the theoretical formulas was derived to account for the production error.

References

1. Carral S., Vergez C., Nederveen C.J. (2011), *Toward a Single Reed Mouthpiece of the Oboe*, Archives of Acoustics, **36**, 2, 267–282.
2. Erkut C., Karjalainen M., Huang P., Välimäki V. (2002), *Acoustical Analysis and Model-Based Sound Synthesis of the Kantele*, Journal of the Acoustical Society of America. **112**, 4, 1681–1691.
3. Fouilhe E., Goli G., Houssay A., Stoppant G. (2011), *Vibration Modes of the Cello Tailpiece*, Archives of Acoustics, **36**, 4, 741–759.
4. Gere J.M., Goodno B.J. (2009), *Mechanics of Materials*, Cengage Learning, 7th Edition, United States of America.
5. Hopkin B. (1996), *Musical Instrument Design*, See Sharp Press, 7^{th} Printing, Arizona, United States.
6. Ismail A., Samad S.A., Hussain A., Azhari C.H., Zainal M.R.M. (2006), *Analysis of the Sound of the Kompang for Computer Music Synthesis*, 4th Student Conference on Research and Development (SCOReD 2006), IEEE, pp. 95–98, Malaysia.
7. Lohri A., Carral S., Chatziioannou V. (2011), *Combination Tones in Violin*, Archives of Acoustics, **36**, 4, 727–740.
8. Marasan R. (2003), *Alat Muzik Sompoton Negeri Sabah* [in Malay], Pejabat Kebudayaan dan Kesenian Negeri Sabah, Sabah, Malaysia.
9. Merriman M. (1924), *Mechanics of Materials*, John Wiley & Sons, 10^{th} Edition, New York, London.
10. Morse P.M. (1948), *Vibration and Sound*, McGraw-Hill Book Company, Inc, 2nd Edition, United States.
11. Ong C.W., Dayou J. (2009), *Frequency Characteristic of Sound from Sompoton Musical Instrument*, Borneo Science, **25**, 71–79.
12. Rujinirum C., Phinyocheep P., Prachyabrued W., Laemsak N. (2005), *Chemical Treatment of Wood for Musical Instruments. Part I: Acoustically Important Properties of Wood for the Ranad (Thai Traditional Xylophone)*, Wood Science and Technology, **39**, 1, 77–85.
13. Skrodzka E.B., Hojan E., Proksza R. (2006), *Vibroacoustic Investigation of a Batter Head of a Snare Drum*, Archives of Acoustics, **31**, 3, 289–297.
14. Skrodzka E., Lapa A., Linde B.B.J., Rosenfeld E. (2011), *Modal parameters of two complete guitars differing in the bracing pattern of the soundboard*, Journal of Acoustical Society of America, **130**, 4, 2186–2194.
15. Someya S., Okamoto K. (2007), *Measurement of the Flow and Its Vibration In Japanese Traditional Bamboo Flute Using the Dynamic PIV*, Journal of Visualization, **10**, 4, 397–404.